

## Interannual Variability of Atmospheric Heat Source/ Sink over the Qinghai–Xizang (Tibetan) Plateau and its Relation to Circulation<sup>①</sup>

Zhao Ping (赵平) *PAZ A*

*Department of Geophysics, Peking University, Beijing 100871*

Chen Longxun (陈隆勋)

*Chinese Academy of Meteorological Sciences, Beijing 100081*

(Received November 10, 1999; revised June 9, 2000)

### ABSTRACT

Based on the 1961–1995 atmospheric apparent heat source / sink and the 1961–1990 snow–cover days and depth over the Qinghai–Xizang Plateau (QXP) and the 1961–1995 reanalysis data of NCEP / NCAR and the 1975–1994 OLR data, this paper discusses the interannual variability of the heat regime and its relation to atmospheric circulation. It is shown that the interannual variability is pronounced, with maximal variability in spring and autumn, and the variability is heterogeneous horizontally. In the years with the weak (or strong) winter cold source, the deep trough over East Asia is to the east (or west) of its normal, which corresponds to strong (or weak) winter monsoon in East Asia. In the years with the strong (or weak) summer heat source, there exists an anomalous cyclone (or anticyclone) in the middle and lower troposphere over the QXP and its neighborhood and anomalous southwest (or northeast) winds over the Yangtze River valley of China, corresponding to strong (or weak) summer monsoon in East Asia. The summer heat source of the QXP is related to the intensity and position of the South Asia high. The QXP snow cover condition of April has a close relation to the heating intensity of summer. There is a remarkable negative correlation between the summer heat source of the QXP and the convection over the southeastern QXP, the Bay of Bengal, the Indo–China Peninsula, the southeastern Asia, the southwest part of China and the lower reaches of the Yangtze River and in the area from the Yellow Sea of China to the Sea of Japan.

**Key words:** Qinghai–Xizang Plateau, Apparent heat source / sink, Snow cover, OLR

### 1. Introduction

The Asian monsoon is greatly influenced by the thermal contrast between the Indian ocean and the Asian continent including the large-scale prominence such as the QXP. Flohn (1957) indicated that the seasonal variation of elevated heating from the QXP surface and anti-phase relationship between north–south temperature and pressure gradients to the south of 35°N play a role in inducing the changes of the East Asian circulation and the Indian monsoon onset. Yeh and Zhang (1974) examined the effects of the QXP thermal function and its induced convection on the maintenance of the South Asia high. Chen et al. (1991) showed that during the break of Indian monsoon, an upper-air anticyclone often emerges over the middle QXP and more rainfall occurs in the south of the QXP. Using monthly data during

<sup>①</sup>This work was supported under the auspices of the National (G1998040800) and CAS's Key Project for Basic Research on the Tibetan Plateau (KZ951–A1–204; KZ95T–06).

July 1972–August 1973, Li et al. (1982) studied atmospheric heat sources in the years of strong and weak summer Indian monsoon. They discovered that in the year of the strong monsoon, the atmosphere has a strong center in the Bay of Bengal and a heat sink in the QXP. In the year of the weak monsoon, a strong heating center is still in the Bay, but a sub-maximal center is in the QXP. Through investigating the structure of the atmospheric heat source and the energy budget over the QXP in the summer of 1979, Chen et al. (1985) indicated that the heat source occurs mainly in the period with much rainfall and the heat sink, except over the eastern QXP, happens during the break of the monsoon. Huang (1985) investigated the effect of the QXP anomalous heat source on atmospheric circulation of the Northern Hemisphere. Yanai et al. (1992) pointed out that the sensible heat flux and radiation cooling over the QXP are responsible for the maintenance of the horizontal temperature gradients that make a large scale thermally-driven vertical circulation to be maintained over the plateau. Using the 1983–1992 data of sounding stations of China, Luo and Zhu (1995) calculated the heat conditions of the eastern QXP during summer half-year and discussed the relation between the heat source and the rainfall of China. They discovered that when the heat source of the QXP intensifies, the rainfall increases in the upper reaches of the Yangtze River and the Huaihe River valley and decreases in the southeast of China. Li and Yanai (1996) calculated the 1979–1992 atmospheric heat and moisture source/sink of the QXP and analyzed the interannual variation of the Asian summer monsoon related to land-sea thermal contrast.

This paper discusses the interannual variability of the QXP atmospheric heat source/sink and its relation to atmospheric circulation, snow cover and OLR.

## 2. Computational method and data

The heat source/sink for a given air column is defined as

$$\langle Q_1 \rangle = F_{sh} + R_{net} + H_{lp}, \quad (1)$$

where  $F_{sh}$  is the surface sensible heat flux,  $R_{net}$  the atmospheric net radiation, and  $H_{lp}$  the precipitation-released latent heat.  $\langle Q_1 \rangle$  is called the heat (or cold) source when it is  $>0$  (or  $<0$ ).

Following Zhao and Chen (2000a,b) and Zhao (1999), we compute the  $\langle Q_1 \rangle$  monthly averages of the QXP during 1961–1995. The QXP in this study is the area with  $\geq 3000$  m topographic height except for that west of  $90^\circ\text{E}$ , north of  $33^\circ\text{N}$ . The used data also include the 1961–1990 monthly snow cover depth and days from the 148 stations (figure omitted) over the QXP and its vicinity, 1961–1995 monthly reanalysis of NCEP/NCAR with  $2.5^\circ \times 2.5^\circ$  resolution, and 1975–1994 monthly OLR with  $2.5^\circ \times 2.5^\circ$  resolution (1978 and 1988 data are missing).

## 3. Features of $\langle Q_1 \rangle$ interannual variability over the QXP

The deviation coefficient is applied in showing the monthly  $\langle Q_1 \rangle$  variability. The coefficient is defined as follows:

$$C_{va} = \frac{1}{|\bar{x}|} \sqrt{\frac{1}{n} \sum_{i=1}^n (x_i - \bar{x})^2},$$

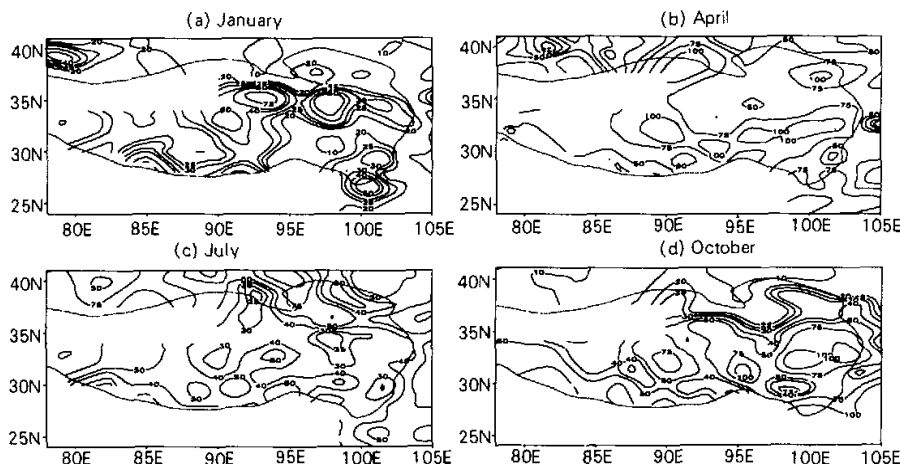


Fig. 1.  $C_{vn}$  (%) of the monthly QXP  $\langle Q_1 \rangle$  during 1961–1995 (dotted line shows the QXP with 300 m height, the same below).

in which  $x_i$  is a time sequence ( $i=1, 2, \dots, n$ ) and all other notations are usual in a meteorological context. By the use of 1961–1995 monthly mean  $\langle Q_1 \rangle$  data we calculate the deviation coefficient  $C_{vn}$  for each month. Figure 1 shows the  $C_{vn}$  distributions for January, April, July, and October. In January (Fig. 1a) the  $C_{vn}$  value exceeds 10% almost all over the QXP and even 30% in the southwest part of the QXP, the middle and the Bayan Har and A Nyêmaqên Mountains of the eastern QXP and the eastern Kunlun Mountains. Its maximum of about 80% occurs in the eastern Kunlun Mountains and the minimum of 7% emerges at  $31^\circ\text{N}$ ,  $97^\circ\text{E}$ . In April (Fig. 1b) the values of the QXP exceed 50% in general. The value above 75% covers the regions from the Tangula Mountains to the mountains of western Sichuan and in the northeastern QXP. A relatively low-value area goes along the Himalayas. In comparison with April, the  $C_{vn}$  value of summer is somewhat smaller. In July (Fig. 1c) the  $C_{vn}$  value is larger than 30% practically all over the QXP, particularly larger than 75% in the western QXP, and also exceeds 50% in the valleys of the Yarlung Zangbo River and the Qaidam basin. The value begins to increase again in October (Fig. 1d). Further examination (figures omitted) also shows that the  $\langle Q_1 \rangle$  variability is quite large in other months. Thus, the interannual variability of the QXP  $\langle Q_1 \rangle$  is large and heterogeneous horizontally.

#### 4. Flow fields in the years of strong and weak winter cold source

##### 4.1 Composite winter cold source

From the 1961–1995 temporal variation of  $\langle Q_1 \rangle$  averaged over the QXP (figures omitted) we select six years separately with a strong and weak winter cold source as follows.

The years of a weak cold source: 1961, 1962, 1964, 1983, 1986, 1989;

The years of a strong cold source: 1966, 1967, 1969, 1970, 1977, 1994.

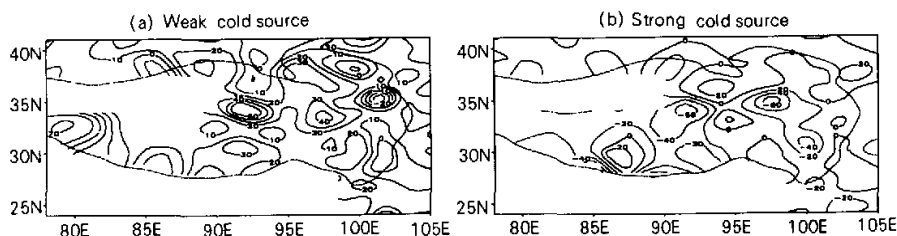


Fig. 2. Composite anomalous  $\langle Q_1 \rangle$  in the six years with a weak and strong winter cold source. Units:  $\text{W m}^{-2}$ .

Figure 2 shows the distribution of the composite  $\langle Q_1 \rangle$  anomalies in the six years separately with a strong and weak winter cold source. One can see that in the years of the weak cold source (Fig. 2a) practically all the QXP is under the control of positive anomalies except for the Qilian Mountains of the northeastern QXP covered by pronounced negative anomalies. The  $\langle Q_1 \rangle$  values above  $20 \text{ W m}^{-2}$  occur mainly in the southwestern QXP and some of the Tanggula and Bayan Har Mountains, around Lhasa (at  $29.7^\circ\text{N}$ ,  $91.1^\circ\text{E}$ ) and Damxung (at  $30.5^\circ\text{N}$ ,  $91.1^\circ\text{E}$ ), particularly in Shiquanhe (at  $32^\circ\text{N}$  and  $79^\circ\text{E}$ ) and Tuotuo Heyan (at  $34^\circ\text{N}$ ,  $92^\circ\text{E}$ ) where the anomalies exceed  $50 \text{ W m}^{-2}$ . In the strong case the composite distribution (Fig. 2b) shows a roughly opposite situation to the weak one. In the strong years negative anomalies cover the QXP except for Lhazê (at  $29.1^\circ\text{N}$ ,  $87.6^\circ\text{E}$ ) and Golmud (at  $36.4^\circ\text{N}$ ,  $94^\circ\text{E}$ ), with the minimums below  $-60 \text{ W m}^{-2}$  appearing in the Himalayas, some parts of the Tanggula and Bayan Har Mountains.

#### 4.2 Composite circulation

Figure 3 shows the composite anomalous wind fields at 850, 500 and 200 hPa in the six years of a weak and a strong cold source of winter. In the weak case, at 850 hPa (Fig. 3a) an anomalous cyclone is south of the QXP, with its center being in the north of the Indian peninsula, while an anomalous anticyclone is northeast of the QXP, with its center being near Lake Baikal. Meanwhile, anomalous west winds prevail in the region from the Arabian Sea to the east of the South China Sea. The east or northeast winds prevail over the region from the mainland of China to Japan, which corresponds to the strong winter monsoon in East Asia. The 500 hPa pattern (Fig. 3b) has rough similarity to the 850 hPa one. A quite strong anomalous cyclone appears at 500 hPa over the QXP, with its two centers being separately in the west and east of the QXP. At 200 hPa (Fig. 3c), the cyclone is still seen and there are two anomalous wavetrains separately in the extratropics and subtropics of the Northern Hemisphere. Three anomalous anticyclonic centers of the extratropical wavetrain appear near Lake Baikal and in the northeastern QXP and between the west of North America and west Europe in turn. Its three cyclonic centers emerge in the Urals and the east of North America and the mid-eastern Pacific in turn. The subtropical wavetrain has the phase opposite to the above one. In the years of strong winter cold source, at 850 hPa (Fig. 3d) an anomalous anticyclone is located to the south of the QXP and a weak anomalous cyclone emerges southeast of the QXP. A large-scale anomalous cyclone covers the area from the northeastern QXP to the extratropical western Pacific, with its two centers separately appearing to the east of Lake Baikal and in the Pacific west of the Aleutians. Anomalous south winds appear over the

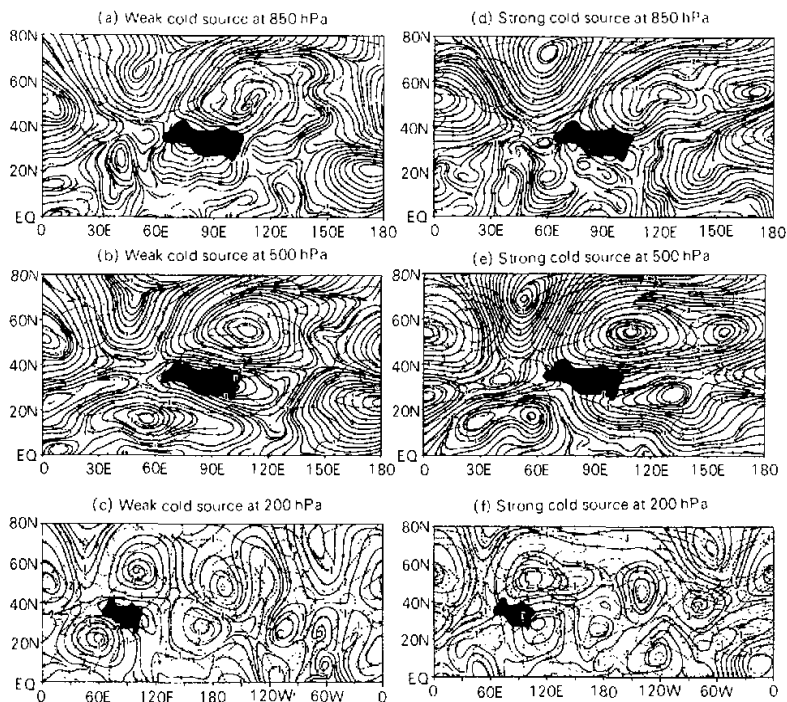


Fig. 3. Composite anomalous streamline at 850, 500 and 200 hPa in the six years separately with a strong and weak winter cold source (The shaded area is the QXP; dashed line is isotach, Unit:  $\text{m/s}$ ).

mainland of China and anomalous west winds prevail over the region from the north of China to Aleutians, which corresponds to the weak winter monsoon in East Asia. The 500 hPa features (Fig. 3e) are quite analogous to those at 850 hPa. In the meantime, a wavetrain also occurs over the extratropics at 200 hPa (Fig. 3f) and has the phase opposite to extratropical one in the years of a weak cold source.

## 5. Flow fields in the years of strong and weak summer heat source

### 5.1 Composite summer heat source

Similar to that of winter, we select the years separately with a strong and weak summer heat source as follows.

The years of strong heat source: 1962, 1974, 1980, 1984, 1987 and 1993;

The years of weak heat source: 1967, 1972, 1975, 1977, 1978 and 1986.

Figure 4 shows the distribution of the composite  $\langle Q_1 \rangle$  anomalies in the six years separately with a strong and weak summer heat source. It is seen that in the years of the summer strong heat source (Fig. 4a) the  $\langle Q_1 \rangle$  values above  $20 \text{ W m}^{-2}$  emerge in the eastern QXP south of  $35^\circ\text{N}$ , with their central values appearing around Nyingchi (at  $29.6^\circ\text{N}$ ,  $94.5^\circ\text{E}$ ) and Litang (at  $30^\circ\text{N}$ ,  $100.2^\circ\text{E}$ ). The anomalies over the southwestern QXP are unremarkable. In the years of the weak heat source (Fig. 4b), except Xainza (at  $30.9^\circ\text{N}$ ,

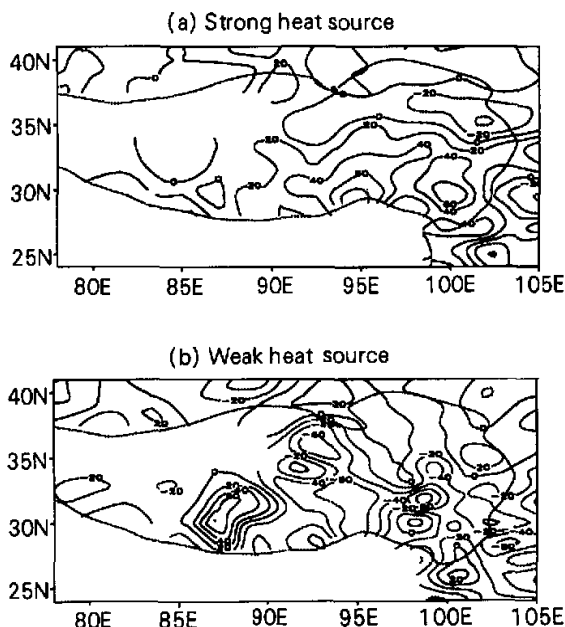


Fig. 4. Composite anomalous  $\langle Q_1 \rangle$  in the six years separately with a weak and strong summer heat source. Units:  $\text{W m}^{-2}$ .

88.6°E) and Lhazê (at 29.1°N, 87.6°E) having noticeable positive anomalies, the QXP is dominated by negative anomalies. Sog county (at 31.9°N, 93.8°E) has the minimum of  $-71 \text{ W m}^{-2}$  and the anomalies over the western QXP also are unremarkable.

## 5.2 Composite circulation

The anomalous wind fields are given at different levels separately for a strong and weak QXP heat source in Fig. 5. It is seen from Fig. 5 that in the strong case, an 850 hPa (Fig. 5a) anomalous cyclone surrounds the plateau and anomalous southwest winds prevail over the region from the Indo-China Peninsula to the mainland of China, corresponding to stronger southwest winds there (namely strong summer monsoon), which is helpful to the transportation of moisture there. An anomalous cyclone and anticyclone separately emerge over the subtropical central Pacific and the eastern Pacific. These features are also seen at the 500 hPa level (Fig. 5b). Over the area from Iran via the plateau to the Bohai Sea of China at 500 hPa there is an anomalous cyclone that still surrounds the plateau in general. From the 100 hPa level the anomalous circulation over the QXP begins to differ from the lower-level counterparts and to 70–50 hPa the circulation becomes opposite to that of lower levels. At 50 hPa (Fig. 5c) the QXP is under the impact of a large-scale anomalous anticyclone centered northwest of the QXP, a pattern that is also seen at 70 hPa (figure omitted). Therefore, a strong summer QXP heat source over the plateau is associated with a strong South Asia high at 70 and 50 hPa that is located to the west of its normal. In the years of the weak heat source, at the 850 hPa (Fig. 5d) level, on the whole, there is an anomalous anticyclone encircling the plateau and an anomalous anticyclone in the middle latitudes of the Pacific west of the

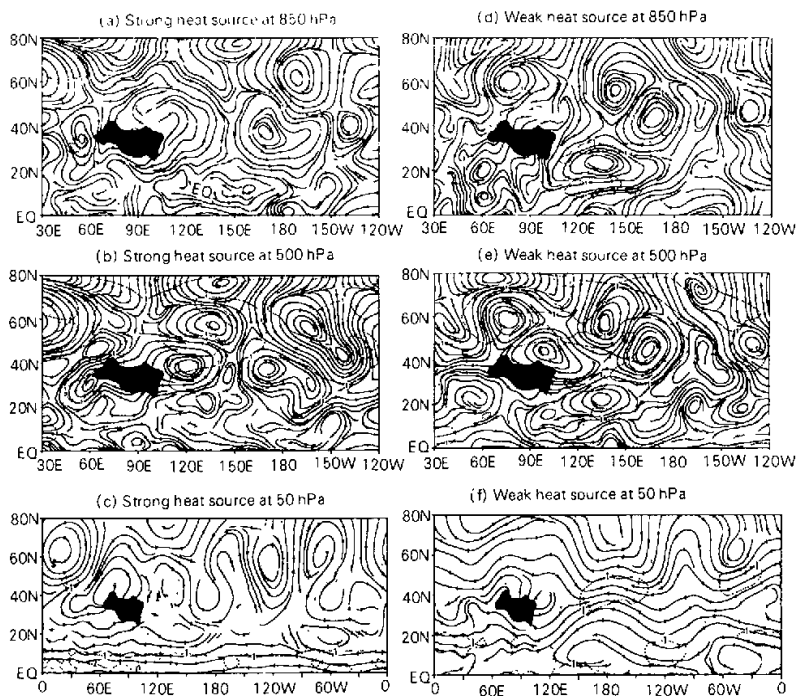


Fig. 5. Composite anomalous streamline at 850, 500 and 50 hPa in the six years separately with a strong and weak summer heat source (The shaded areas is the QXP; dashed line is isotach, Unit:  $m/s$ ).

dateline. Anomalous northeast winds appear over the mainland of China, which corresponds to weak southwest winds, namely weak summer monsoon. This is in contrast to that in the strong case. The features at 850 hPa in the weak case are also displayed at 500 hPa (Fig. 5e) except that an anomalous anticyclone over the QXP is centered northeast of the plateau and an anomalous cyclone is even more pronounced in the subtropical eastern Pacific. The 50 hPa features (Fig. 5f) in a weak case greatly differ from those of a strong heat source, particularly in the middle of the QXP and the extratropics north of the plateau where the anomalous winds are opposite to the strong case. To the northeast of the QXP is an anomalous anticyclone that favours the South Asia high to lie east of its normal.

Additionally, in the years with a strong heat source, at 50 hPa (Fig. 5f) there is a wavetrain consisting of three anomalous anticyclones and as many anomalous cyclones in the Northern Hemisphere. Of these anticyclones, one stretches from the Iranian highland via the QXP to the Japanese islands with its centers separately around the Iranian highland and Vladivostok; the other two are centered separately in the extratropical eastern Pacific and northeastern Canada. The three anomalous cyclonic centers are separately situated in the midlatitude of the western Pacific, the western coasts of North America and northwestern Europe. A 50 hPa anomalous easterly is also seen throughout low latitudes globally, with

anomalous east winds above  $2 \text{ m s}^{-1}$  appearing in the middle of Africa and the equatorial Indian Ocean and around the equator of South America. In the weak case, anomalous west winds stretch from Africa to the equatorial eastern Pacific, with no noticeable wavetrain emerging in the extratropics of the Northern Hemisphere.

From the above analysis, one can see that in the years of a strong (or weak) heat source of the QXP, there is an anomalous cyclone (or anticyclone) in the middle and lower troposphere over the QXP and its adjacent areas, strong (or weak) southwest winds over the mainland of China and an anomalous anticyclone (or cyclone) in the subtropical eastern Pacific; a low-level anomalous anticyclone (or cyclone) covers the region from the South China Sea to the western Pacific; the middle and lower reaches of the Yangtze River is under the effect of anomalous southwest (or northeast) winds that can transport more (or less) moisture to there and cause more (or less) rainfall, which corresponds to the strong (or weak) summer monsoon in East Asia. A strong (or weak) equatorial easterly takes place in the stratosphere. The intensity of the QXP summer heat source has close relation to the intensity and position of South Asia high. The effect of the heat source on the high is not so remarkable at 100 hPa as at 70 and 50 hPa.

## 6. Relation between the QXP heat source and snow

We separately calculate the correlation coefficient between the monthly anomalous  $\langle Q_1 \rangle$  values and snow depth/days over the QXP during 1961–1990. The results show that the  $\langle Q_1 \rangle$  values of spring, autumn and winter are in weak correlation with the previous snow cover depth/days. But the  $\langle Q_1 \rangle$  of summer is correlated remarkably with the snow day and depth of April (Table 1), their correlation coefficients are separately  $-0.55$  and  $-0.49$ , passing test at 99% significance level. Further examination shows that the negative correlation between the spring QXP depth/days and summer QXP latent heat of condensation exceeds  $-0.60$  that passes test at 99.9% significance level. Because the latent heat is a main contributor of the QXP  $\langle Q_1 \rangle$ , the abundant snowfall of April melts in subsequent months, resulting in the weak QXP heat source and a weaker QXP monsoon that causes less summer rainfall and weaker summer  $\langle Q_1 \rangle$  over the QXP. In addition, the analysis shows (figures omitted) that there is no remarkable correlation between the summer heat source and previous atmospheric circulation. We also compute correlation coefficients between the monthly heat source of the QXP and Eurasian snow cover from NOAA satellite observations for 1967–1990. The correlation is unremarkable except the positive correlation (only passing test at 90% significance level) between the Eurasian snow cover of March/April and the QXP summer heat source.

**Table 1.** Correlation coefficients of the QXP summer  $\langle Q_1 \rangle$  to snow cover depth (SCD) and snow cover days (SCDs) of the QXP

	J	F	M	A	M	J	J	A	S	O	N	D
SCDs	-0.11	-0.24	-0.01	-0.55★	-0.13	-0.17	-0.20	-0.07	-0.12	-0.15	0.15	0.26
SCD	0.07	-0.23	-0.39☆	-0.49★	-0.14	0.02	0.01	0.03	0.09	-0.04	0.04	-0.13

Note that the negative correlation denoted by ☆ (or ★) passes test at 95% (or 99%) significance level.

As a result, the anomaly of atmospheric circulation in winter firstly affects spring snow conditions of the QXP probably and then affects the heat source of summer there. A stronger



(or weaker) summer heat source of the QXP follows the greater (or shallower) snow depth and more (or less) snow days of April over the QXP.

## 7. Relation of $\langle Q_1 \rangle$ to OLR

Figure 6 shows the distribution of correlation coefficients between the QXP summer heat source and the summer OLR during 1975–1994 (the 1978 and 1988 observations were not included in default of data). The negative correlation passing test at 95% significance level is seen in the southeastern QXP, the Bay of Bengal, the Indo–China Peninsula, the southeastern Asia, the southwest part of China and the lower reaches of the Yangtze River. Their central values pass test at 99% significance level. The negative correlation also emerges in the area from the Yellow Sea of China to the Sea of Japan, with its central values passing test at 99% significance level. Additionally, we notice that the European continent displays remarkable negative correlation (passing test at 95% significance level), with its maximums passing test at 99% significance level, which is probably related to energy transportation by the wavetrain of the extratropics of the Northern Hemisphere that has been discussed in Section 5. Very weak correlativity between the  $\langle Q_1 \rangle$  and OLR is seen in the western Pacific “warm pool” (in  $0^\circ$ – $20^\circ$ N,  $130^\circ$ E– $160^\circ$ E).

## 8. Summary and discussion

Using the monthly QXP atmospheric heat sources/sinks, snow cover depth/days, OLR and NCEP/NCAR reanalysis data, this paper investigates the relationship of the QXP heat regime to Asian monsoons and the QXP snow cover. We arrive at the following conclusions.

(1) The QXP  $\langle Q_1 \rangle$  has remarkable interannual variability for each month, especially in spring and autumn. The variability is heterogeneous horizontally. In winter the  $\langle Q_1 \rangle$

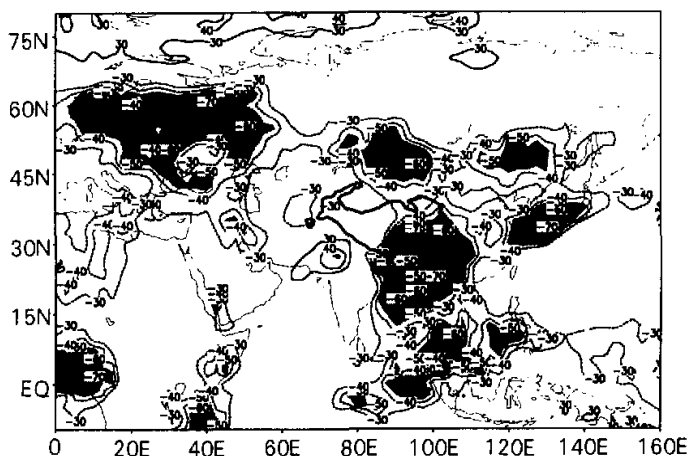


Fig. 6. Correlation coefficients ( $\times 100$ ) between summer QXP  $\langle Q_1 \rangle$  and OLR during 1975–1994 (Thick dotted line is the QXP; the shaded areas pass test at 95% significance level).

difference between the years of a strong and a weak cold source lies largely in the southwestern QXP and the Tanggula and Bayan Har Mountains of the eastern QXP. In summer the difference between the years of a strong and weak heat source occurs mainly in the eastern QXP. This feature is likely related to the complicated terrain and conditions of the underlying surface as well as the changeable circulation systems there.

(2) The QXP weak (or strong) cold source corresponds to a low-level anomalous cyclone (or anticyclone) south of the QXP and around Lake Baikal and over the Urals. This pattern is related to the East Asian deep trough lying to the east (or west) of normal, which causes winter cold air to go southward east (or west) of  $105^{\circ}\text{E}$  and anomalous north (or south) winds to the east of the QXP and south (or north) winds to the north of the QXP, corresponding to strong (or weak) winter monsoon in East Asia, not favoring (or favoring) the movement of cold air into the QXP and producing the warm (or cool) temperature there. Thus, the winter monsoon anomaly in East Asia is associated with the intensity of winter cold source over the QXP.

(3) In the years of a strong (or weak) heat source of the QXP, there is an anomalous cyclone (or anticyclone) in the middle and lower troposphere over the QXP and its adjacent areas, and strong (or weak) southwest winds over the mainland of China, corresponding to strong (or weak) summer monsoon in East Asia and more (or less) precipitation in the Yangtze River valleys. Strong (or weak) equatorial east winds take place in the stratosphere. The intensity of summer heat source is also related to the intensity and position of South Asia high, but the effect of the heat source on the high is more remarkable at 70 and 50 hPa.

(4) The QXP snow cover of April is in remarkable correlation with the  $\langle Q_1 \rangle$  intensity of subsequent summer. The more (or less) snow cover days and greater (or shallower) depth in April are followed by a weak (or strong) heat source of summer. The anomaly of winter atmospheric circulation probably affects the summer QXP heat source by means of spring snow conditions there.

(5) The summer heat source of the QXP has remarkable negative correlation with the convection over the southeastern QXP, the Bay of Bengal, the Indo-China Peninsula and the southeastern Asia. This is due to the fact that the latent heat of precipitation is a main contributor to the summer heat source of the QXP so that the negative correlation is remarkable. The negative correlation also emerges in the southwest part of China and the lower reaches of the Yangtze River and in the area from the Huang Sea of China to the Sea of Japan, which is probably related to the frequent eastward movement of the low-value systems produced over the QXP. Very weak correlativity between the  $\langle Q_1 \rangle$  and OLR is seen in the western Pacific "warm pool".

#### REFERENCES

- Chen Longxun et al., 1985: The features of atmospheric heat source variation and energy budget over the Qinghai-Xizang plateau in the summer of 1979. *Acta Meteorologica Sinica*, **43**(2), 208–220 (in Chinese).
- Chen Longxun, Zhu Qiangen, and Luo Huibang, 1991: *East Asian Monsoons*, China Meteorological Press, Beijing, 62–76 (in Chinese).
- Flohn, H., 1957: Large-scale aspects of the "summer monsoon" in South and East Asia. *J. Meteor. Soc. Japan* (75th Ann. Vol.): 180–186.
- Huang Ronghui, 1985: Effects of anomaly of atmospheric heat sources over the Tibetan plateau on the anomaly of northern atmospheric circulation. *Acta Meteorologica Sinica*, **43**(2), 208–220 (in Chinese).
- Li Chenfeng, and M. Yanai, 1996: The onset and interannual variability of the Asian summer monsoon in relation to

- land-sea thermal contrast. *J. Climate*, **9**(2), 358-375.
- Li Weiliang, Chen Longxun, and Jin Zuhui, 1982: The structures of mean circulation and distribution of heat source over Asia and the western Pacific during strong and weak Indian monsoon. Proceedings of the symposium on the summer monsoon in the southeastern Asia (1981), People's Press of Yunnan Province, Yunnan, 74-84 (in Chinese).
- Luo Huibang, and Zhu Rong, 1995: The effects of the atmospheric heat source anomaly over the eastern Qinghai-Xizang plateau during summer half-year on the circulation and rainfall. *Meteorological Science and Technology*, **15**, 94-102 (in Chinese).
- Yanai, M., Li Chenfeng, and Song Z., 1992: Seasonal heating of the Tibetan plateau and its effects on the evolution of the Asian summer monsoon. *J. Meteor. Soc. Japan*, **70**(1), 319-351.
- Yeh Tucheng, and Zhang Jieqian, 1974: Preliminary simulation of the heating effects of the Tibetan plateau on summer atmospheric circulations in East Asia. *Science in China* (Series B), **3**(3), 301-320 (in Chinese).
- Zhao Ping, 1999: The heat regime over the Qinghai-Xizang plateau and its relationship with air and ocean. Ph.D. thesis of Chinese Academy of Meteorological Sciences, Beijing, 124-155 (in Chinese).
- Zhao Ping, and Chen Longxun, 2000a: Study on climatic features of surface turbulent heat exchange coefficients and surface thermal source over the Qinghai-Tibetan Plateau. *Acta Meteorologica Sinica*, **14**(1), 13-29.
- Zhao Ping, and Chen Longxun, 2000b: Calculation of solar albedo and radiation equilibrium over the Qinghai-Xizang Plateau and analysis of their climatic features. *Advances in Atmospheric Sciences*, **17**(1), 140-156.

## 青藏高原大气热量源汇年际变化 及其与大气环流的关系

赵 平 陈隆勋

### 摘 要

本文使用 1961~1995 年逐月青藏高原地区大气视热量源汇  $<Q1>$  资料、1961~1990 年青藏高原地区积雪日数和积雪深度资料、美国 NCEP/NCAR 的再分析资料以及 1975~1994 年全球 OLR 资料, 讨论了高原大气热状况年际变化及其与大气环流的关系, 发现: 高原地区大气热源年际变化明显, 其中春季和秋季高原地区  $<Q1>$  的变率最大, 并且水平分布很不均匀; 当冬季高原冷源弱(或强)时, 东亚大槽位置偏东(或西), 对应着东亚强(或弱)的冬季风; 夏季高原热源强(或弱)的年份, 在高原及其邻近地区的对流层中、低层为偏差气旋环流(或反气旋环流), 在中国长江流域低层为异常的西南风(或东北风), 对应着东亚强(或弱)的夏季风, 夏季高原热源强度还与南亚高压的强度和位置有关; 春季 4 月的积雪状况与夏季高原大气热源强度有明显关系; 夏季高原热源与同期青藏高原东南部、孟加拉湾、中南半岛、东南亚、中国西南部、长江流域和从黄海到日本海一带对流有明显正相关。

关键词: 青藏高原, 视热量源汇, 积雪, OLR